Journal of The Electrochemical Society

OPEN ACCESS

Chemical Preparation of Metallic Cu Layer on Glass Substrate Using Intermediate $Cu(OH)_2$/Cu(O, S) Bilayer

To cite this article: Haruka Shimizu *et al* 2022 *J. Electrochem. Soc.* **169** 122506

Journal of The Electrochemical Society, 2022 **169** 122506

Chemical Preparation of Metallic Cu Layer on Glass Substrate Using Intermediate $Cu(OH)_2$/Cu(O, S) Bilayer

Haruka Shimizu, Junji Sasano, Pei Loon Khoo,* and Masanobu Izaki*,z

Graduate School of Engineering, Toyohashi University of Technology, 1-1 Hibarigaoka, Tempaku-cho, Toyohashi-shi, Aichi 441-8580 Japan

A metallic Cu layer with a sheet resistance of 0.19 Ω was chemically prepared on a glass substrate by chemical reduction of the intermediate $Cu(OH)_2$/Cu(O,S) bilayers using dimethylamine-borane (DMAB), while $Cu(OH)_2$, and Cu(O,S) layers were fabricated by a sequential chemical bath deposition (CBD) in aqueous solutions containing copper (II) nitrate hydrate and ammonium nitrate with urea and thiourea. The thickness of the $Cu(OH)_2$ and resultant Cu layers were strongly affected by the structure under the Cu(O, S) layer, and a metallic Cu layer was formed mainly from the $Cu(OH)_2$ layer. The reduction reactions of $Cu(OH)_2$ and Cu(O, S) were discussed based on thermodynamics.

 [DOI: 10.1149/1945-7111/aca724]

Manuscript submitted September 28, 2022; revised manuscript received November 15, 2022. Published December 23, 2022.

Supplementary material for this article is available online

Over the past few decades, social network service (SNS) and on-demand content streaming services using wireless communication tools through applications in smartphones and tablets have become increasingly popular channels of entertainment, in addition to the deployment of massive internet of things (IoT) systems in enterprises and factories with embedded sensors communicating via cloud computing systems, resulting in a significant increase in data traffic. 5 G mmWave (30 c 100 GHz in frequency) provides the potential due to the high speed, large capacity, low latency, and high-density communication.[1]

Glass sheets have attracted increasing attention as the substrate for System-in-Package (SiP) and Antenna-in-Package (AiP) in utilizing the performance of 5 G mmWave due to their suitable coefficient of thermal expansion, low dielectric constant, low hygroscopic properties, and low surface roughness to reduce transmission loss, an alternative to conventional polymer substrates such as a glass-epoxy resin substrate.[2–4] The Cu circuits in SiP and AiP have been fabricated by electroless Cu plating technique with a Pd catalyst,[5] and additional insertions of metal oxides such as SiO_2 and metal layers such as Cu, Ti, and W prepared by chemical solution and vacuum processes[6,7] have been implemented to enhance the adhesion strength of the Cu layer on glass substrates.

Chemical bath deposition (CBD) is a chemical solution process for preparing metal oxides and sulfides by shifting the solubility curve by increasing the solution temperature,[8,9] which has been used in the preparation of CdS[10] and Zn(S, O, OH)[11] to be installed in Cu(In,Ga)Se_2 and Cu_2SnZnS_4(CZTS) solar cells as buffer layers. Cu (O, S) layers could also be prepared by CBD, with the adhesion to the glass substrate attributed to the metal-oxygen-metal bonding at the heterointerface.[12] Preparation of metallic Cu layers with low resistivity and sufficient adhesivity have been reported, prepared by a chemical reduction of copper oxide layers.[13]

Here, we report the chemical preparation of metallic Cu layer on glass substrates using intermediate $Cu(OH)_2$/Cu(O, S) bilayers prepared by chemical bath deposition (CBD) in a Cu-NH_3- complex aqueous solutions containing urea and thiourea. The resulting Cu layer prepared on the glass substrates by chemical reduction of mainly $Cu(OH)_2$ in a dimethylamine-borane (DMAB) aqueous solution possessed a low electrical resistance of 0.19 Ω and adequate adhesivity without peeling off.

Experimental

The Cu(O, S) layers were prepared on glass substrates by simple immersions in an aqueous solution containing 0.05 mol l^{-1} copper (II) nitrate hydrate, 0.05 mol l^{-1} ammonium nitrate, and 5.6 mmol l^{-1} thiourea at 343 K, with varying deposition time from 5 to 30 min. The $Cu(OH)_2$ layers were also deposited by simple immersions in aqueous solutions containing 0.05 mol l^{-1} copper(II) nitrate hydrate, 0.05 mol l^{-1} ammonium nitrate, and 5.6 mmol l^{-1} urea at 333 K for 15 min, on bare glass or on Cu(O, S)/glass substrates priorly prepared. The chemical reduction was performed by simple immersion in a 0.01 mol l^{-1} dimethylamine-borane (DMAB) aqueous solution at 303 K. The reduction areas of the $Cu(OH)_2$ and $Cu(OH)_2$/Cu(O, S) layers were limited by masking to the 1 cm × 1 cm center part of the films with an adhesive tape (NITTO DENKO Corporation, NITOFRON Glass Adhesive tape 973UL), which was then removed by peeling from the substrate after the reduction processes. The solutions were prepared by using reagent-grade chemicals and distilled water purified by a MilliPore Ellix-UV-Advantage. Conventional soda-lime glass sheets were used as the substrates after rinsing in acetone for 30 s.

X-ray diffraction patterns were recorded by an X-ray diffractometer (Rigaku RINT 2500) with a monochromated CuKα radiation operated at 40 kV and 200 mA. The field-emission transmission electron microscopy (FE-TEM) observation was performed with JEOL JSM2100F at an accelerating voltage of 200 kV for which samples were prepared by using a focused ion beam (FIB, Hitachi FB2000). The surface and cross-sectional structures were observed with a field-emission scanning electron microscope (FE-SEM, Hitachi, SU8000). The sheet resistance was estimated with a four-point probe tester with a probe distance of 1 mm at 300 K.

Results and Discussion

Effects of the underlying Cu(O,S) layer on the structure and growth of upper $Cu(OH)_2$.—The appearance of $Cu(OH)_2$ layer and $Cu(OH)_2$/Cu(O,S) bilayers prepared for 5, 10, 15, 20, and 30 min-Cu(O, S) deposition on the glass substrate before and after chemical reductions were shown in Fig. 1. The $Cu(OH)_2$ layer showed a light blue appearance, while the $Cu(OH)_2$/Cu(O, S) layers showed a dark blue to black appearance with an increase in Cu(O, S) deposition time. The underlying Cu(O,S) layer which was composed of Cu, O, and S elements as shown in the electron spectra in Fig. S1, is a p-type semiconductor with 1.35 eV in bandgap energy,[12] which contributed to the dark and black appearances. The appearance after the chemical reduction is further described later.

*Electrochemical Society Active Member.
zE-mail: m-izaki@me.tut.ac.jp

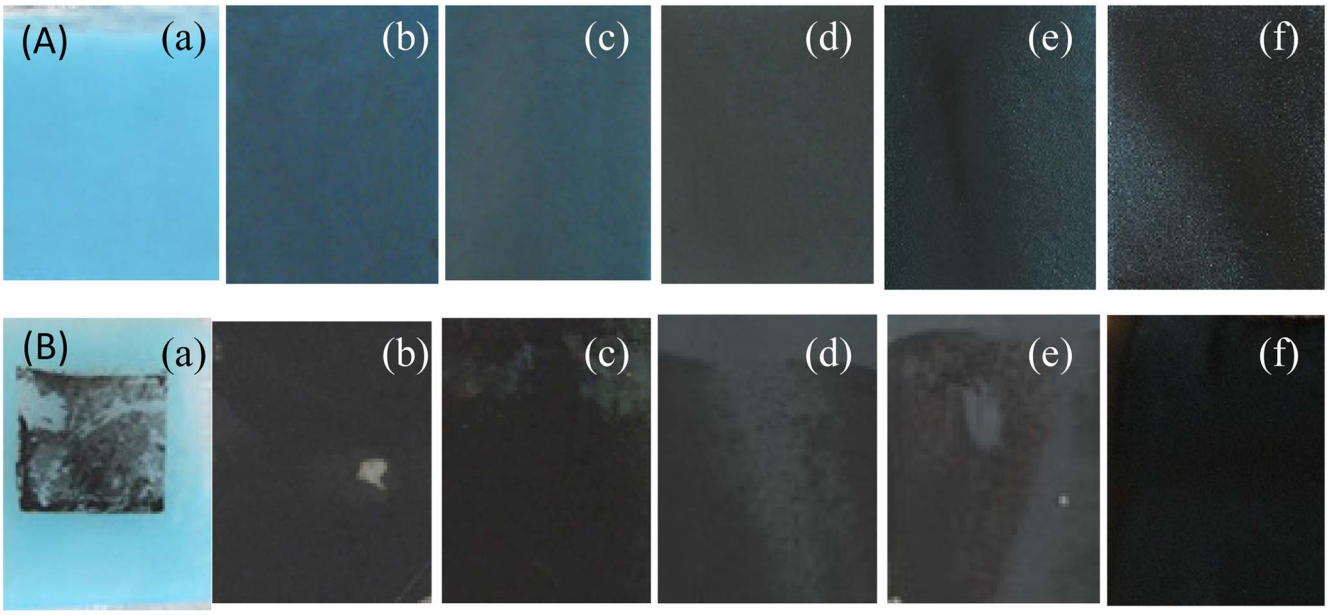

Figure 1. Appearances of $Cu(OH)_2$ layer (a) and $Cu(OH)_2$/Cu(O,S) bilayers prepared for 5 (b), 10 (c), 15 (d), 20 (e), and 30 min (f)—Cu(O,S) deposition before (A) and after chemical reduction (B) by DMAB.

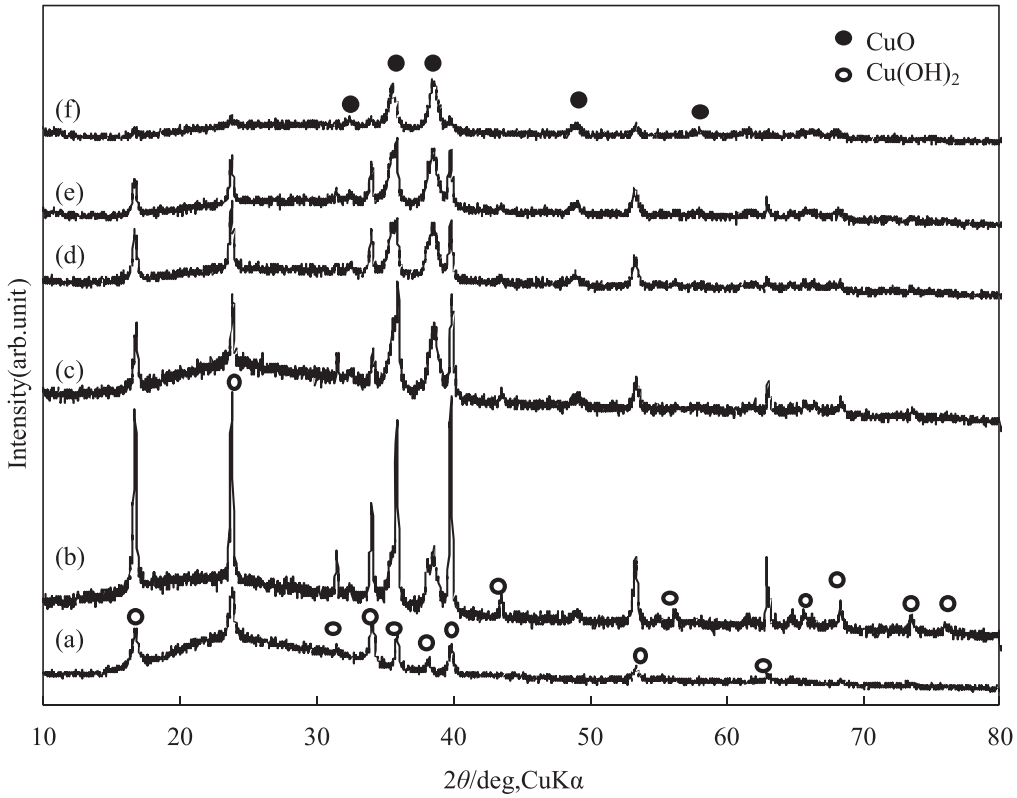

Figure 2. X-ray diffraction patterns for $Cu(OH)_2$ layer (a) and $Cu(OH)_2$/Cu(O,S) bilayers prepared for 5 (b), 10 (c), 15 (d), 20 (e), and 30 min (f)—Cu(O,S) deposition time.

Figure 2 shows the X-ray diffraction patterns for $Cu(OH)_2$ and $Cu(OH)_2$/Cu(O, S) bilayers prepared with 5, 10, 15, 20, and 30 min for the Cu(O, S) deposition. Fifteen diffracted X-ray peaks represented by unfilled circles were observed for the $Cu(OH)_2$ layer prepared for 15 min (Fig. 2a), in addition to the broadened peak at around 20–30 degrees originated from the glass substrate, and these peaks were identified as those for the $Cu(OH)_2$ with a characteristic orthorhombic lattice,[14] and no other peaks could be observed on the pattern. The X-ray diffraction patterns were almost the same in peak angles for the $Cu(OH)_2$ layers prepared for 5 to 30 min as shown in Fig. S2, although the peak intensities increased with the increase in deposition time. The peak angles, width, and intensity ratios of $Cu(OH)_2$ peaks were almost constant, irrespective of the insertion of Cu(O, S) and the deposition time, but the intensity was strongly affected by the presence of Cu(O, S). All the $Cu(OH)_2$ peaks were strengthened by the insertion of the Cu(O, S) layer for 5 min

compared to that of a single $Cu(OH)_2$ layer, but the intensity decreased dramatically with the increase in Cu(O, S) deposition time to 30 min, suggesting a change in the $Cu(OH)_2$ layer thickness depending on the Cu(O, S) deposition time.

The appearance of additional peaks at around 35.5, 38.8, and 48.6 degrees was confirmed for the all the $Cu(OH)_2$/Cu(O,S) bilayers, and were identified as (002) and/or (11$\underline{1}$), (111) and/or (200), and (20$\underline{2}$) peaks for CuO with a characteristic monoclinic lattice.[15] it was difficult to distinguish the crystal plane due to the close d-values for (002)/(11$\underline{1}$), and (111)/(200) planes. The intensity of the CuO peaks increased with the increase in Cu(O, S) deposition time to 10 min, and then showed almost constant intensity.

Figure 3 shows the surface and cross-section images for $Cu(OH)_2$ layer and $Cu(OH)_2$/Cu(O,S) bilayers prepared for 5, 10, 15, 20, and 30 min in Cu(O, S) deposition. The $Cu(OH)_2$ layer (Fig. 3a) prepared for 15 min was composed of randomly dispersed columnar grains grown from the glass substrate and voids were observed between the columnar grains on the surface and also near the glass substrate. The columnar grains possessed a characteristic radiated multi-plate cross-sectional morphology with a size of approximately 0.88 μm, with ten or more thin, single plates radially developed outwards from the center of the columnar grain. The average thickness of the $Cu(OH)_2$ layer was estimated to be approximately 1.98 μm. The grain morphology of the $Cu(OH)_2$ layers was similar to those prepared for 5 to 30 min, and the thickness increased with the increase in deposition time up to 15 min, which possessed an almost constant value of approximately 2 μm, as shown in Fig. S3.

Both the upper $Cu(OH)_2$ and bottom Cu(O, S) layers could be clearly observed for all the $Cu(OH)_2$/Cu(O,S) bilayers fabricated with 5 to 30 min for the Cu(O,S) depositions. The Cu(O,S) layers prepared for 5 and 10 min were composed of granular grains, and defects such as pores and voids could not be observed throughout the Cu(O, S) layer or near the heterointerface to the glass substrate. The average thickness of the $Cu(OH)_2$ and Cu(O, S) layers estimated from the SEM images were summarized in Fig. S4. The thicknesses were obtained by averaging ten measurements due to the irregularities of the surface and interface. The average thicknesses of the Cu (O, S) layers were estimated to be 0.78 μm, and 0.95 μm for 5, and 10 min, respectively. Also, the Cu(O,S) layers prepared over 15 min were composed of granular grains and elongated thorn-like grains with lengths of 0.9–1.6 μm and widths of 63–93 nm which were additionally grown radially from the granular grain layer. The granular layer of the Cu(O, S) layers showed an almost constant thickness of around 1.3 μm above 15 min, excluding the thorn-like grains.

The FE-TEM images for the Cu(O,S) layer prepared for 30 min on a glass substrate were shown in Fig. S1. The Cu(O, S) layer was composed of an upper dendritic layer possessing a large surface irregularity and a bottom granular grain layer. The bottom layer was composed of granular Cu(O, S) grains with sizes of 6.3–7 nm, and the layer adhered to the glass substrate without any defects such as pores or space, as shown in the magnified image (Fig. S1b). The thorn-like grains observed in Fig. 3 correspond to the dendrite grains shown in Fig. S1. Such dendritic and thorn-like grains were also observed for the CuO layer prepared by electrodeposition in a Cu-NH_3-complex aqueous solution,[16] and by thermal oxidation of a metallic Cu sheet.[17]

The Zn(S, O, OH) layer prepared by CBD in a Zn-NH_3-complex aqueous solution possessed a layered structure composed of an upper $Zn(OH)_2$-rich layer and a bottom Zn(O, S) layer. The bottom Zn(O, S) layer was formed due to a supersaturation condition originating from the low solubility product of ZnS at the initial stage, with the subsequent $Zn(OH)_2$-rich layer deposited on the Zn(O, S) layer under the condition of supersaturation with a relatively large solubility product of $Zn(OH)_2$, according to the solubility curves for $Zn(OH)_2$, ZnO, and ZnS.[9,11] Since the Cu(O, S) layer prepared by the CBD process was reported to be Cu-O-S solid solution containing 1 mol % sulfur,[12] the involvement of CuS was considered. The solubility products (*Ksp*) of $Cu(OH)_2$ and CuS were reported to be 2.2×10^{-20} and 5×10^{-36}, and the solubility product of CuO was slightly larger than that of $Cu(OH)_2$, showing a similar tendency to those for $Zn(OH)_2$, ZnO, and ZnS.[8,9] In addition, since the structure and solution formulation for the Zn(S, O, OH) layer was similar to those for the Cu(O, S) layer, it is being speculated that

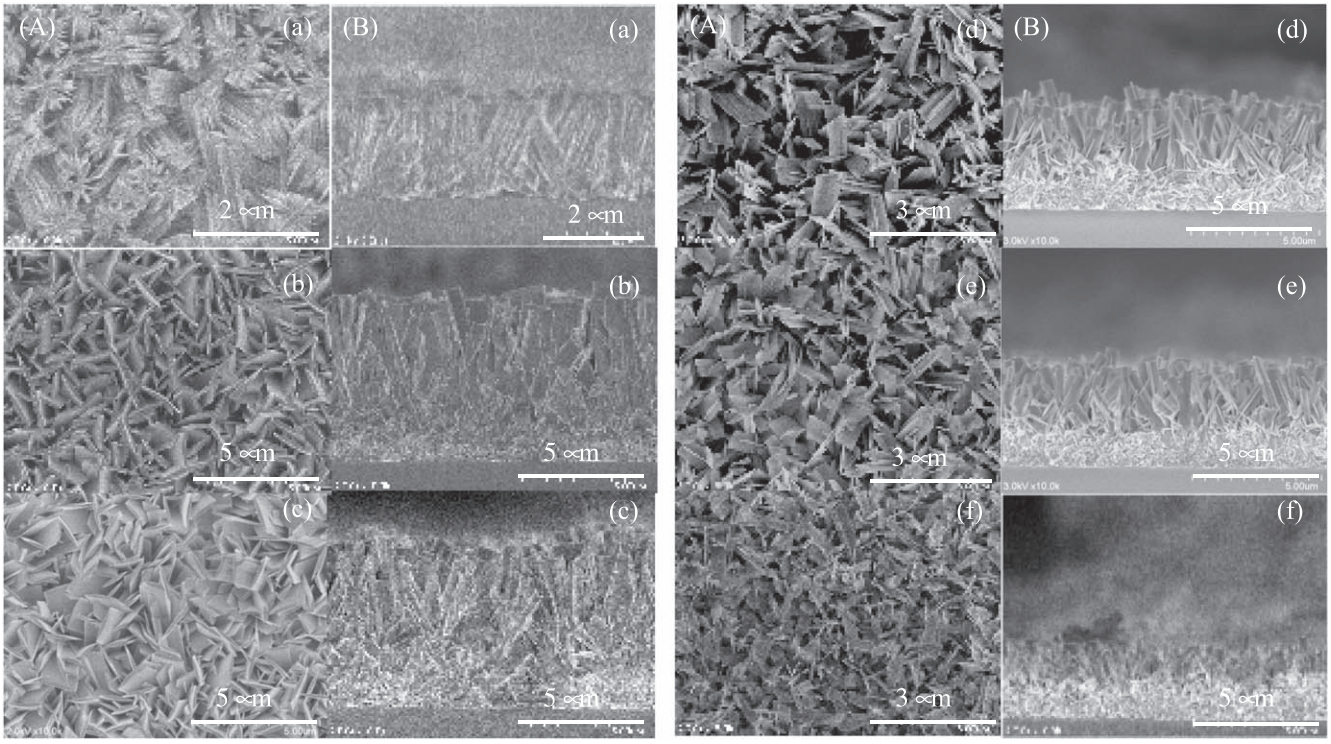

Figure 3. Surface (A) and cross section images (B) for $Cu(OH)_2$ layer (a) and $Cu(OH)_2$/Cu(O,S) bilayers prepared for 5 (b), 10 (c), 15 (d), 20 (e), and 30 min (f)—Cu(O,S) deposition.

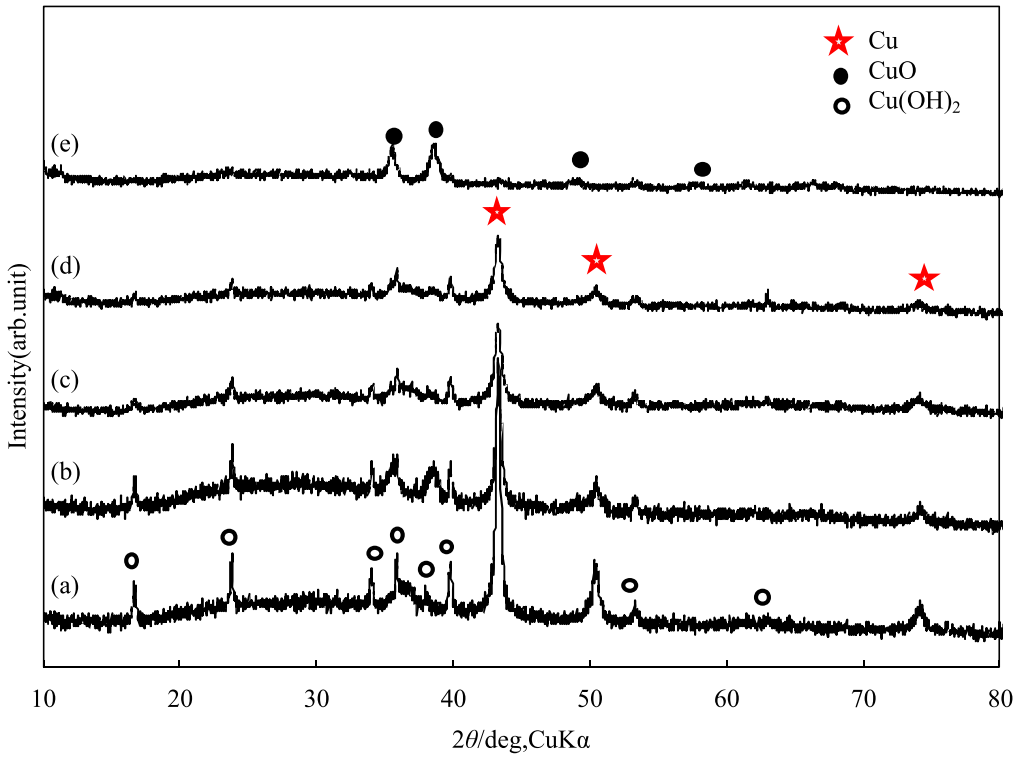

Figure 4. X-ray diffraction patterns for $Cu(OH)_2$/Cu(O,S) bilayers prepared for 5 (a), 10 (b), 15 (c), 20 (d), and 30 min (e)—Cu(O,S) deposition time after chemical reduction.

the structure and composition between the bottom granular Cu(O, S) layer and upper dendrite grains were different.

The growth of the upper $Cu(OH)_2$ layer was strongly affected by the insertion and structure of the lower Cu(O, S) layer. The average thickness of the $Cu(OH)_2$ layers increased from 1.98 to 5.9 μm by introducing the Cu(O, S) layer prepared for 5 min, and the cross-sectional morphology of the $Cu(OH)_2$ columnar grains changed from the radiating multi-plates to single-plates. The average thickness of the $Cu(OH)_2$ layer decreased to 5.6 μm for 10 min and then to 1.56 μm for 30 min, as shown in Fig. S4, and was consistent with the intensity change of the diffracted X-ray peaks originating from $Cu(OH)_2$. The change in the average thickness is related to the structural change of Cu(O, S) layers. The single plate $Cu(OH)_2$ columnar grains showed a decrease in width from 1.6 to 0.70 μm, and in thickness of 0.64 to 0.047 μm with the increase in Cu(O, S) deposition time as shown in Figs. 3A 3b–3f, while keeping the morphology of single-plates. Thick $Cu(OH)_2$ layers were obtained on the granular Cu(O, S) grain layer, and the decrease in thickness and single-plate size occurred on the Cu(O, S) layer with thorn-like grains.

Since there is no lattice relationship between $Cu(OH)_2$ and the glass substrate, the nucleation occurred under a condition where the interaction with the glass substrate was very weak, followed by the growth of nuclei. On the contrary, although the lattice relationship between the monoclinic Cu(O, S) and orthorhombic $Cu(OH)_2$ lattices was not clear, the bottom granular Cu(O, S) grains provided nucleation sites for the growth of $Cu(OH)_2$, resulting in the increase in $Cu(OH)_2$ thickness and change in grain morphology. However, on the Cu(O, S) layer with thorn-like grains, the thickness of the $Cu(OH)_2$ layers decreased, indicating growth suppression. The difference in structure and composition between the granular Cu (O, S) layer and the thorn-like grains aforementioned may be a reason for the change in the growth of the upper $Cu(OH)_2$ layer.

Metallic Cu layer formation by chemical reduction.—The appearances of the $Cu(OH)_2$ layer and $Cu(OH)_2$/Cu(O, S) bilayers fabricated for 5–30 min-Cu(O, S) deposition after the chemical reduction using dimethylamine-borane (DMAB) are shown in Fig. 1. The appearance of the $Cu(OH)_2$ layer changed from light blue to black after the chemical reduction, but the black-colored substances were easily peeled off from the glass substrate by rinsing with water, indicating their poor adhesion to the glass substrate, as shown in the center square black part in Figs. 1B, 1a. A slight change in appearance could be observed for all the $Cu(OH)_2$/Cu(O, S) bilayers, but no peeling could be observed, irrespective of the Cu (O, S) deposition time. Thus, further investigations were performed only on the $Cu(OH)_2$/Cu(O, S) bilayers.

Figure 4 shows the X-ray diffraction patterns of $Cu(OH)_2$/Cu(O, S) bilayers fabricated in which the Cu(O, S) were deposited 5–30 min after the chemical reduction. The diffracted X-ray peaks assigned as Cu(111), (200), and (220) planes appeared at 43.56, 50.36, and 73.96 degrees due to the chemical reduction, in addition to the peaks originating from $Cu(OH)_2$ and Cu(O, S). The Cu peaks showed a strong intensity for 5 min which weakened with the increase in the Cu(O,S) deposition time. The Cu peaks with very weak intensities were detected for 30 min, and the X-ray diffraction pattern was almost the same in profile and peak angles as that before the chemical reduction. Since the intensity ratios of the Cu peaks were almost constant irrespective of the Cu(O,S) deposition time, the intensity change was related to the Cu layer thickness. The lattice constant of the Cu estimated from the peak angles was 0.360 nm for the a-axis for 5–20 min-Cu(O, S) depositions, which value was close to the reported standard value of 0.3615 nm.[18] The intensities of both the Cu(O, S), and $Cu(OH)_2$ peaks decreased after the chemical reduction for 5 to 20 min Cu(O, S) depositions compared to those before the chemical reduction, except for the 30 min-Cu(O, S) deposition.

Figure 5 shows the surface and cross-sectional images for the $Cu(OH)_2$/Cu(O, S) bilayers fabricated for 5 to 30 min Cu(O, S) depositions after chemical reduction. Aggregation of granular Cu grains with the size of approximately 61 nm formed over the entire surface for 5 and 10 min Cu(O, S) depositions by chemical reduction, while plate-like $Cu(OH)_2$ columnar grains were less observed throughout the upper layer. Since the X-ray diffraction

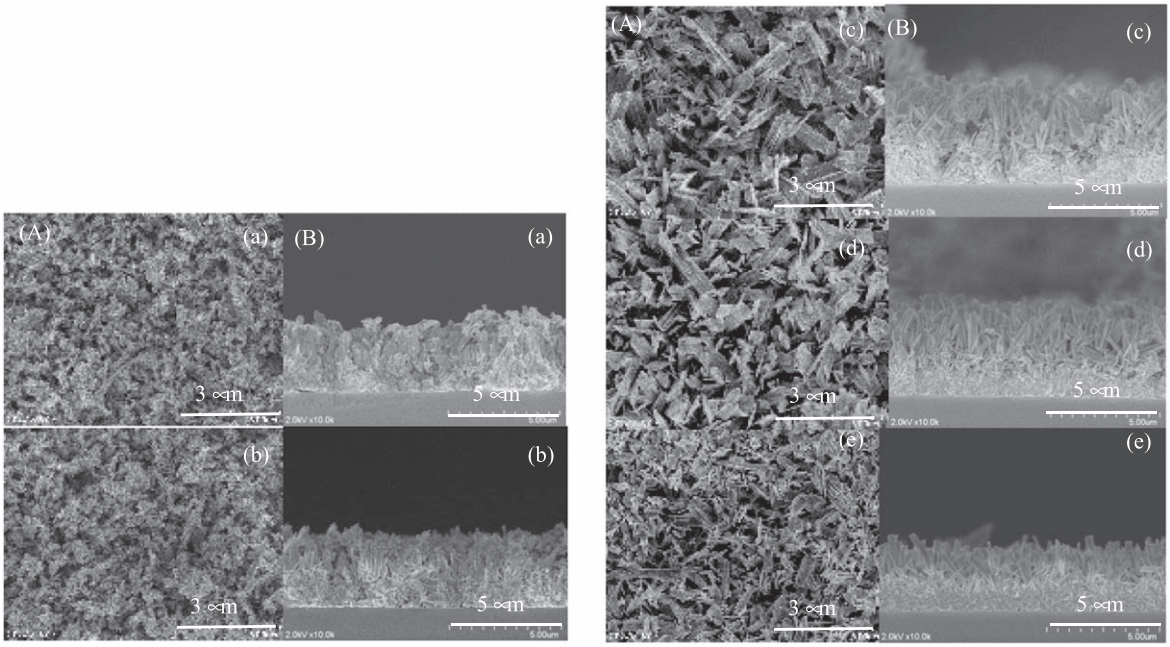

Figure 5. Surface (A) and cross section images (B) for $Cu(OH)_2$/Cu(O,S) bilayers prepared for 5 (a), 10 (b), 15 (c), 20 (d), and 30 min (e)—Cu(O,S) deposition time after chemical reduction.

patterns showed some remaining $Cu(OH)_2$ even after the chemical reduction, this indicated that the upper layer was a mixture of metallic Cu and $Cu(OH)_2$ components. The upper layer thicknesses were reduced to 2.7 μm and 2.6 μm after the chemical reduction from 5.9 μm and 5.6 μm. The Cu(O,S) layers were observed between the upper layer and glass substrate, and the average thicknesses were estimated to be 0.43 μm and 0.79 μm for the 5 and 10 min Cu(O, S) depositions, which slightly decreased from 0.78 μm and 0.95 μm after the chemical reduction. The plate-like $Cu(OH)_2$ grain morphology remained after reductions above 15 min-Cu(O, S) depositions, but the smooth and flat surface of the plate grains changed into a slightly rough surface with granular Cu grains. The thicknesses of the upper layer were estimated to be 3.0 μm, 2.8 μm, and 1.6 μm for 15, 20, and 30 min-Cu(O, S) depositions after the chemical reduction, and these values almost agreed with those before the chemical reduction. The Cu(O, S) layer was clearly observed between the upper layer and glass substrate, and the thickness was an almost constant value of 1.3 μm, which was similar to that before chemical reduction. It was speculated that the chemical reduction of $Cu(OH)_2$ to metallic Cu was limited at the surface of the plate-like $Cu(OH)_2$ grains at depositions longer than 15 min-Cu(O, S). The effects of the Cu(O, S) layer on the growth of the $Cu(OH)_2$ grains changed with a boundary at around 10–15 min-Cu(O,S) deposition. Although further investigation on the detailed structural analysis and consideration of the growth is needed, it was clear that the Cu(O, S) layer and its structure strongly affected the growth of the upper $Cu(OH)_2$ grains and the reduction behavior.

$Cu(OH)_2$, CuO, and Cu possess crystal systems of an orthorhombic lattice with a = 0.5256 nm, b = 1.0593 nm,[14] c = 0.2347 nm, and Z = 4, monoclinic lattice with a = 0.46883 nm, b = 0.34229 nm, c = 0.51319 nm, β = 99.506 degrees, and Z = 4,[15] and cubic lattice with a = 0.3615 nm and Z = 4,[18] respectively. The volumes of the unit cells were estimated to be 0.131 nm^3, 0.081 nm^3, and 0.047 nm^3 at Z = 4 for $Cu(OH)_2$, CuO, and Cu. The metallic Cu layer was formed mainly by the reduction of $Cu(OH)_2$ grains, and the shrink in volume after being reduced was estimated to be approximately 65%. The volume reduction roughly estimated from the change in thickness by the chemical reduction was approximately 50% and 56% for 5 and 10 min-Cu(O, S) depositions, and these values were consistent with the theoretical value, despite the approximation on the measurement of the thickness.

The $Cu(OH)_2$ was mainly reduced to metallic Cu by the chemical reduction with DMAB, but the reduction of Cu(O,S) was limited. The reduction reaction and the standard Gibb's energy for the reactions for $Cu(OH)_2$, CuO, and CuS are described and calculated using the chemical potentials of each chemical substance as follows:[9,16,19]

$$Cu(OH)_2 + 2H^+ + 2e \rightleftarrows Cu + 2H_2O,\ \Delta_r G^0 = -225.2\ \text{kJ mol}^{-1}$$

$$CuO + 2H^+ + 2e \rightleftarrows Cu + H_2O,\ \Delta_r G^0 = -107.4\ \text{kJ mol}^{-1}$$

$$CuS + H^+ + 2e \rightleftarrows Cu + HS^-,\ \Delta_r G^0 = 65.7\ \text{kJ mol}^{-1}$$

Since the information on the thermodynamic property of dimethylamine-borane (DMAB) used as the reducing agent in this study was inadequate, BH_4^- anion was used as an alternative consideration. The oxidation reaction and standard Gibb's energy for the reaction of BH_4^-/BO_2^- can be mentioned as follows:[13,20–23]

$$BO_2^- + 8H^+ + 8e \rightleftarrows BH_4^- + 2H_2O,\ \Delta_r G^0 = 319.0\ \text{kJ mol}^{-1}$$

The reaction schemes and the standard Gibb's energy for the reactions of $Cu(OH)_2$, CuO, and CuS with reducing agent BH_4^- are speculated as follows;

$$4Cu(OH)_2 + BH_4^- \rightleftarrows 4Cu + BO_2^- + 6H_2O,\ \Delta_r G^0 = -1219.4\ \text{kJ mol}^{-1}$$

$$4CuO + BH_4^- \rightleftarrows 4Cu + BO_2^- + 2H_2O,\ \Delta_r G^0 = -748.7\ \text{kJ mol}^{-1}$$

$$4CuS + BH_4^- + 2H_2O \rightleftarrows 4Cu + BO_2^- + 4H^+,\ \Delta_r G^0 = -56.3\text{kJ mol}^{-1}$$

The reduction reactions of $Cu(OH)_2$, CuO, and CuS by BH_4^- will occur spontaneously at an equilibrium state, but compared to $Cu(OH)_2$ and CuO, CuS was relatively difficult to be reduced, according to the values of standard Gibb's energy for the reactions. It was also speculated that Cu(O, S) was relatively difficult to be reduced by DMAB compared to the CuO species with the incorporation of S impurities, and this may be the reason for some remaining Cu(O, S) in the layer after the chemical reduction.

Figure 6 shows the sheet resistance and resistivity of Cu/$Cu(OH)_2$/Cu(O, S) layers prepared for 5–30 min-Cu(O, S)

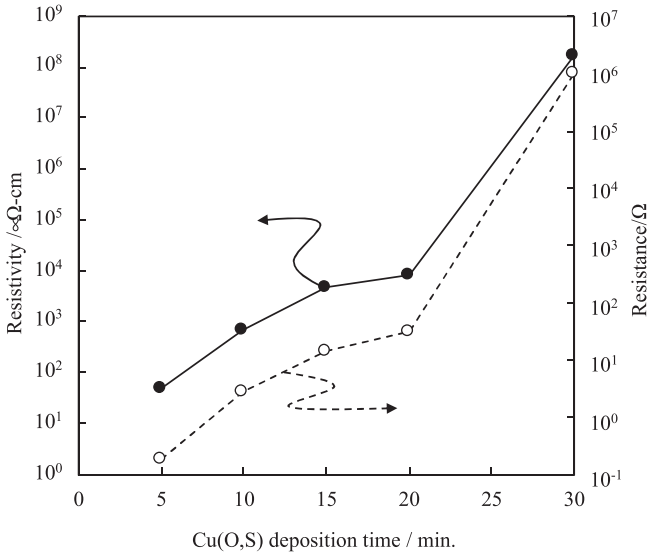

Figure 6. Resistivity and resistance for $Cu(OH)_2$/Cu(O,S) bilayers prepared for 5, 10, 15, 20, and 30 min—Cu(O,S) deposition time after chemical reduction.

depositions. The resistivity was calculated from the sheet resistance and Cu layer thickness, with the assumption that the upper layer is composed of mainly metallic Cu. The lowest resistance of 0.19 Ω was obtained for the Cu layer prepared on a glass substrate with an intermediate $Cu(OH)_2$/Cu(O,S) bilayer fabricated from the 5 min-Cu (O, S) deposition. The resistance increased dramatically to an order of 10^6 Ω, which was close to the resistance of a CuO layer,[24] with the increase in Cu(O, S) deposition time to 30 min. In short, the thickness of the Cu layer decreased with an increase in Cu(O, S) deposition time, and the resistance showed a dependency on the thickness. The lowest resistivity of 51 $\mu\Omega-$cm was obtained at 5 min-Cu(O, S) deposition time, which value was much higher than 1.71–4.60 $\mu\Omega-$cm for electrodeposited Cu layers and 1.7–4.1 $\mu\Omega-$cm for electroless Cu layers.[25] The Cu layers prepared by chemical reduction contained some amount of $Cu(OH)_2$ and was composed of granular grains with small grain size around 60 nm, which contributed to a high resistivity.

Conclusion

The $Cu(OH)_2$/Cu(O, S) bilayers were fabricated on soda-lime glass substrates by sequential chemical bath deposition (CBD) in aqueous solutions containing copper (II) nitrate hydrate, and ammonium nitrate with urea and thiourea, and the metallic Cu layer was formed by the chemical reduction with a dimethylamine-borane (DMAB) with adequate adhesion. The thicknesses of the $Cu(OH)_2$ layer were strongly affected by the structure of the bottom Cu(O, S) layer. The metallic Cu layer was chemically formed mainly from the $Cu(OH)_2$ layer, and the bottom Cu(O, S) layer remained after the chemical reduction, resulting in the formation of Cu/$Cu(OH)_2$/Cu(O, S) on the glass substrates. The Cu layer formed on a glass substrate with an intermediate $Cu(OH)_2$/Cu(O, S) bilayer fabricated for 5 min-Cu(O, S) deposition revealed a resistance of 0.19 Ω, which increased with an increase in Cu(O, S) deposition time. The results here demonstrated a Pd-free chemical solution process for fabricating metallic Cu layer on glass substrates, which will benefit future applications in forthcoming technologies for communications.

ORCID

Pei Loon Khoo https://orcid.org/0000-0002-4230-6791
Masanobu Izaki https://orcid.org/0000-0002-3959-1923

References

1. https://qualcomm.com/content/dam/qcomm-martech/dm-assets/documents/Web-Tech_Final_Rising_to_Meet_The_1000x_Mobile_Data_Challenge_102412.pdf.
2. D. H. Levy, S. F. Nelson, A. B. Shorey, and P. Balentine, *Chip Scale Rev.*, **1** (2021).
3. D. H. Levy, S. F. Nelson, A. B. Shorey, and P. Balentine, *2021 IEEE 71st Electro. Comp. Tech. Conf. ECTC*, **2222** (2021).
4. S. Okude, *Fujikura Tech. J.*, **134**, 8 (2021).
5. M. Schlesinger and M. Paunovic, *Modern Electroplating* 5th edition, 433(New York)(Wiley, New Jersey) (2010).
6. Z. Liu, S. Hunegnaw, H. Fu, J. Wang, T. Magaya, M. Merschky, T. Bernhard, A. Shorey, and H. Yun, *International Symposium on Microelectronics*, **2015**, 000365 (2015).
7. Y. Sato, *J. Surf. Fin. Soc. Jpn*, **66**, 33 (2015).
8. G. Hodes, *Chemical Solution Deposition of Semiconductor Films* (New York, Marcel Dekker) 1 (2003).
9. M. Izaki, P. L. Khoo, and T. Shinagawa, *J. Electrochem. Soc.*, **168**, 112510 (2021).
10. D. Lincot and R. O. Borges, *J. Electrochem. Soc.*, **139**, 1860 (1992).
11. M. Izaki, S. Sugiyama, T. Okamoto, Y. Kusano, T. Maki, H. Komaki, H. Shibata, and S. Niki, *Prog. Photovol: Res. Appl.*, **24**, 397 (2016).
12. M. Izaki, Y. Yamane, J. Sasano, T. Shinagawa, and M. Inoue, *Electrochem. Solid Sate Lett.*, **14**, D30 (2011).
13. M. Izaki, Y. Kobayashi, J. Katayama, and S. Ohtomo, *J. Electrochem. Soc.*, **153**, C612 (2006).
14. Joint Committee on Powder Diffraction Standards, Powder Diffraction File; Intensity Data for Diffraction Data: $Cu(OH)_2$, PDF, 01-080-0656.
15. Joint Committee on Powder Diffraction Standards, Powder Diffraction File; Intensity Data for Diffraction Data: CuO, PDF, 00-048-1548.
16. J. G. Speight, *Lange's Handbook of Chemistry* (New York, McGraw-Hill) 16th ed.1 (1976), 9761.
17. M. Izaki, M. Nagai, K. Maeda, B. F. Fariza, K. Motomura, J. Sasano, T. Shinagawa, and S. Watase, *J. Electrochem. Soc.*, **158**, D578 (2011).
18. Joint Committee on Powder Diffraction Standards, Powder Diffraction File; Intensity Data for Diffraction Data: Cu, PDF:00-004-0836.
19. D. D. Wagman, W. H. Evans, V. B. Parker, R. H. Shumm, I. Halow, S. M. bailey, K. L. Churney, and R. L. Nuttall, *J. Phys. Chem. Ref. Data*, **11**, 2 (1982).
20. I. Ohno, O. Wakabayashi, and S. Haruyama, *Denki Kagaku*, **53**, 196 (1985).
21. M. Izaki and T. Omi, *J. Electrochem. Soc.*, **144**, L3 (1997).
22. J. E. A. M. Van Den Meerakker, *J. Appl. Electrochem.*, **11**, 395 (1981).
23. M. Izaki, *Thin Solid Films*, **520**, 2434 (2012).
24. M. Schlesinger and M. Paunovic, *Modern Electroplating* (New York, Wiley) 5th ed., 42, p. 442 (2010).
25. P. Wang, X. Zhao, and B. Li, *Opt. Exp.*, **19**, 11271 (2011).